

## OPTICAL SPECTRA OF CADMIUM SULFIDE THIN FILMS DEVELOPED BY CHEMICAL BATH DEPOSITION TECHNIQUE AT VERY LOW SOLUTION CONCENTRATIONS: AIR-ANNEALING EFFECT

N. NASIR, Z. RIZWAN\*

*Department of Applied Sciences, Faculty of Science National Textile University,  
Sheikhupur Road, 37610 Faisalabad, Pakistan*

The concentration of  $\text{CdCl}_2:(\text{NH}_2)_2\text{CS}=0.00125 \text{ M}:0.0025 \text{ M}$  was used to develop cadmium sulfide (CdS) thin films on commercial glass substrate through chemical bath deposition (CBD) technique, employing  $\text{CdCl}_2$  as a  $\text{Cd}^{2+}$  source while  $(\text{NH}_2)_2\text{CS}$  for  $\text{S}^{2-}$  at constant bath temperature  $71^\circ\text{C}$ . The bonding of the thin films was excellent for all samples. Thin film samples were annealed in air from  $200^\circ\text{C}$  to  $360^\circ\text{C}$  for 60 minutes. The minimum and maximum thickness 31.5 nm, 42 nm was observed at the annealing temperatures  $280^\circ\text{C}$  and  $320^\circ\text{C}$ , respectively. All developed thin films were of cubic phase CdS along with very feeble peaks that belong to hexagonal phase CdS. Size of crystallite developed films was decreased from 46 nm to 14.8 nm and this size increased to 43 nm at higher annealing temperature. Absorption coefficient ( $\alpha$ ), Urbach energy  $E_u$  and Optical  $E_g$  were selected as characterization parameters. The parameters were obtained from transmission spectral records have been taken as the function of temperature. The 97% transmission was best attained for the annealed in air films at  $240^\circ\text{C}$  annealing temperature.

(Received July 14, 2018; Accepted September 12, 2018)

**Keywords:** CBD technique, Thin film, CdS, Air-annealing

### 1. Introduction

There are lot of techniques like vacuum evaporation, molecular beam epitaxy, electro-deposition, pulsed laser evaporation, sputtering, radio frequency, spray pyrolysis deposition, metal vapor organic deposition, successive ionic layer adsorption, close-spaced sublimation and other techniques are being used to grow thin films, since long time. Also chemical bath deposition (CBD) technique is being used since a long time. All these techniques are also being used successfully to develop a CdS thin films. Chemical bath deposition (CBD) is a versatile techniques among all these techniques and attractive technique due to its simplicity [1]. It is also an inexpensive technique. This technique also has special features like, development of large deposition area at very low bath temperature. This technique also have a good control on the development of uniform thin layer. Chemical bath deposition technique is recognized as solution growth technique. This deposition technique of the thin film is also being applied since 1960s [2, 3]. The CBD method also improves the CdS window layer performance when compared with the other thin film deposition techniques. Moreover, the thin films deposited through this technique are made of very closely packed nano-crystals. This feature makes the development of thin films gorgeous for basic as well as practical research of NCs. Maximum efficacy was achieved with this CBD technique in growing CdS thin films as window layer [2-5]. Maximum efficiency was achieved when this CBD method was ensured to develop buffer layer for Cu (In, Ga)Se<sub>2</sub> (CIGS) and CdTe solar cells [5, 6]. Other optoelectronic and electronic devices are also being fabricated by this technique [7, 8]. It is an outstanding heterojunction companion for p-type semiconductor CuInSe<sub>2</sub>, Cu (In, Ga) Se<sub>2</sub>, and CdTe because of its wide optical  $E_g$  (2.42 eV). It is also very significant material because of its unique properties, for example, high electron affinity,

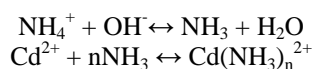
---

\*Corresponding author: zahidrizwan64@gmail.com

photoconductivity and high refractive index i.e. (2.5) [9, 10]. The immersed substrate in an alkaline solution comprising ( $\text{Cd}^{2+}$ ) and ( $\text{S}^{2-}$ ) ions generated by chemical reaction occurring in the aqueous solution to develop the CdS thin film on commercial dipped substrate [11, 12]. Film growing time, temperature of bath, relative concentrations of solution which provide ions of  $\text{Cd}^{2+}$  as well as  $\text{S}^{2-}$  in chemical reaction. Solution pH is necessary for the growth of CdS thin film on dipped substrate in CBD technique.

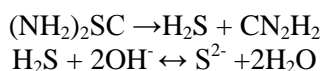
### Chemistry of CdS thin film

The CdS thin films are synthesized using the chemical reaction series [13]. In first step, hydrolyses of cadmium salt generates  $\text{Cd}^{2+}$  ions. To stabilize the  $\text{Cd}^{2+}$  ions, they are allowed to react with ammonia generated by a stabilizer and cadmium n-amino complex was allowed to form.

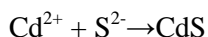


Where n = number of ligands ranging from 1 to 6

In second step, Alkaline hydrolysis of thiourea ( $(\text{NH}_2)_2\text{CS}$ ) is performed in order to get  $\text{S}^{2-}$  through a series of chemical reaction as follows;



In final reaction, finally, the  $\text{Cd}^{2+}$  and  $\text{S}^{2-}$  ions react to make CdS as follows;



In present study, a versatile technique (CBD) has been used to develop nano-structured thin film of CdS on commercial microscopic glass slides. The experiment was performed at low molar concentrations of  $\text{CdCl}_2$  (0.00125) :  $(\text{NH}_2)_2\text{CS}$  (0.0025) and  $\text{CdCl}_2$  (0.0025) :  $(\text{NH}_2)_2\text{CS}$  (0.005). Optical as well as structural properties of CdS thin films have been investigated here as a function of solution concentration and air-annealing temperature 200, 240, 280, 320 and 360 °C.

## 2. Experimental

All used solvents and reagents were of analytical grade.  $(\text{NH}_2)_2\text{CS}$  and  $\text{CdCl}_2$  were purchased from Alfa Aesar. Solvents (99.9% purity) were used in the experiment. Glassware and substrate (commercial microscopic glass slides of size  $76 \times 25 \times 1.2$  mm) dipped for 24 hours in the solution of nitric acid then rinsed with double deionized water. Glassware and substrate dried carefully before the start of experiment. The substrates were further cleaned with ethanol and acetone ultrasonically and then washed with doubly deionized water and dried. The solution concentration named as R =  $\text{CdCl}_2$  (0.00125) :  $(\text{NH}_2)_2\text{CS}$  (0.0025).

Solution concentration (R) were divided into six parts in separate beakers. These beakers were placed, separately in water bath. Solution's temperature was raised upto 71°C by digital hot plate. Ammonia ( $\text{NH}_3$ ) aqueous solution of was used as complexing agent in this experiment.

Aqueous  $\text{NH}_3$  was added slowly in solution of  $\text{CdCl}_2$  to dissolve  $\text{Cd}(\text{OH})_2$  white precipitates on constant stirring. Solution pH was attuned at 11. Solution of thiourea drop by drop was added in  $\text{CdCl}_2$  solution in about 25 seconds under robust stirring condition. Resulting clear-solution temperature was raised to 71 °C. Then cleaned glass substrates were immersed vertically with the help of self-made Teflon holders. The evaporation of ammonia was controlled by covering the solution containers. To ensure the uniform stirring and homogenous mixing throughout, 2 hours deposition process was achieved with the help of stirring of mixture with the help of magnetic bar. Thin film samples were washing deionized  $\text{H}_2\text{O}$  ultrasonically to eliminate particles of CdS which were loosely-adhered. All samples were dried in air at room temperature.

Deposited samples of thin film were grouped into 06 sets. One thin film sample was named as-deposited ( $R_0$ ). Other samples were annealed in air at the temperature 200, 240, 280, 320 and 360 °C for 60 minutes and the samples were named as  $R_{200}$ ,  $R_{240}$ ,  $R_{280}$ ,  $R_{320}$  and  $R_{360}$ , respectively. The heating and cooling rate was 4 °C per minute.

Ellipsometer (DRE-Dr. RISS) with model ELX-02C was used to measure the thickness of the films. X-ray diffraction characterization was carried on using radiation  $\text{Cu}(K_\alpha)$  having 1.540598 Å wavelength using Diffractometer PANalytical with model X'Pert-Pro-(PW1830). X'Pert High Score software was used to analyze crystalline phases in thin film samples. Scherer formula was used to measure the crystallite size ( $D$ ) using Eq. 1;

$$D = \frac{0.94 (\lambda)}{\beta \cos \theta} \quad (1)$$

Here  $\beta$  is the FWHM in radians of diffracted peak. Bragg angle ( $\theta$ ), wavelength ( $\lambda$ ) of x-rays and Scherer constant  $K$  was taken 0.94 to complete numerical calculations [14, 15].

Optical-transmittance data was captured with the Shimadzu (double beam) spectrophotometer with wavelength ( $\lambda$ ) range 350 nm to 1100 nm. The following Eq. 2 was used to determine the absorption coefficient ( $\alpha$ );

$$\alpha = \frac{\ln(\frac{1}{T})}{d} \quad (2)$$

The value of optical  $E_g$  was determined by the absorption coefficient ( $\alpha$ ) using Eq. 3,

$$\alpha = \frac{A(h\nu - E_g)^n}{h\nu} \quad (3)$$

Here is constant ( $A$ ), photon energy ( $h\nu$ ) and  $n=1/2$  for the direct optical  $E_g$  semiconductor material because the CdS is direct  $E_g$  material [16, 17]. The plot of  $(\alpha h\nu)^2$  versus photon energy ( $h\nu$ ) gives the value of  $E_g$ . When the curve was extrapolated as  $(\alpha h\nu)^2 = 0$ . Where  $\alpha$  is absorption coefficient displays a tail of sub-optical  $E_g$ . Urbach-energy ( $E_u$ ), related with tail width, determined from the Eq. 4 [17];

$$\alpha = \alpha_0 e^{h\nu/E_u} \quad (4)$$

where  $\alpha_0$  is constant. Urbach energy ( $E_u$ ) value is obtained using Inverse slop of the plot  $\ln \alpha$  against  $h\nu$ .

### 3. Results and discussion

CdS films developed using cadmium chloride and Thiourea at low solution concentration. All thin films, as-deposited and annealed in air were found polycrystalline in nature [18, 19]. XRD patterns are presented in Fig. 1. The detailed analysis of the x-ray diffraction pattern is discussed here. The scaled XRD graphs are so small in size and many small peaks of the graphs are lost in this process.

The As-deposited sample ( $R_0$ ) shows peaks at angle  $2\theta = 26.7405^\circ$ ,  $44.2257^\circ$ ,  $52.3939^\circ$  and  $54.9616^\circ$  which belongs to (111), (220), (311), (222) planes of cubic phase of CdS, respectively (ref: 01-075-0581). It is observed that a peak at an angle  $2\theta = 28.1468^\circ$  which belongs to the plane (101) that is hexagonal phase of CdS (ref: 01-072-2306).

The sample annealed in air at 200 °C  $R_{200}$  show peaks at an angle  $2\theta = 26.7670^\circ$ ,  $44.4147^\circ$  and  $52.4847^\circ$  are related to the (111), (220) and (311) planes which are cubic CdS, respectively (ref: 01-080-0019). Three very small peaks that are at an angle  $2\theta = 28.7526^\circ$ ,  $58.4426^\circ$  and  $66.6771^\circ$  which belong to planes (101), (202) and (203) that is hexagonal CdS (ref: 00-002-0549).

Samples annealed in air at 240 °C ( $R_{240}$ ) show the peaks at  $2\theta=26.7925^\circ$ ,  $44.2394^\circ$  belongs to planes (111), (220), respectively. These two peaks are related to the cubic phase of CdS (01-075-1546). Two very small peaks at  $2\theta = 28.7302^\circ$ ,  $48.1229^\circ$  are also observed that belong to (101), (103) planes of hexagonal phase of CdS (ref: 00-001-0783).

Samples annealed in air at 280 °C ( $R_{280}$ ) indicates the XRD pattern and peaks at cubic  $2\theta = 26.7862^\circ$ ,  $44.2519^\circ$  and  $52.5012^\circ$ . These peaks belong to (111), (220) and (311) planes of cubic CdS (01-080-0019). Only two peaks at  $2\theta=28.3202^\circ$  and  $48.5256^\circ$  belongs to the planes (101) and (103) (ref. 00-001-0783). These two peaks belong to the hexagonal phase of CdS. The observed peaks for the samples annealed in air at 320 °C ( $R_{320}$ ) at  $2\theta=26.7814^\circ$ ,  $44.0238^\circ$ ,  $52.3565^\circ$ ,  $55.1343^\circ$  and  $72.8184^\circ$  belongs to (111), (220), (311), (222) and (420) planes, respectively. These peaks are related to the cubic phase of CdS (ref. 01-075-0581). Only two peaks at  $2\theta= 28.2638^\circ$  and  $44.0238^\circ$  belongs to (101) and (110) planes. These two peaks are related to the hexagonal phase of CdS (ref. 01-080-0006). Only two very feeble peaks at angle  $2\theta= 32.8947^\circ$  and  $38.1918^\circ$  which belongs to (102) and (200) planes. These two peaks are related to the orthorhombic  $\text{CdSO}_4$  (ref. 01-085-0673).

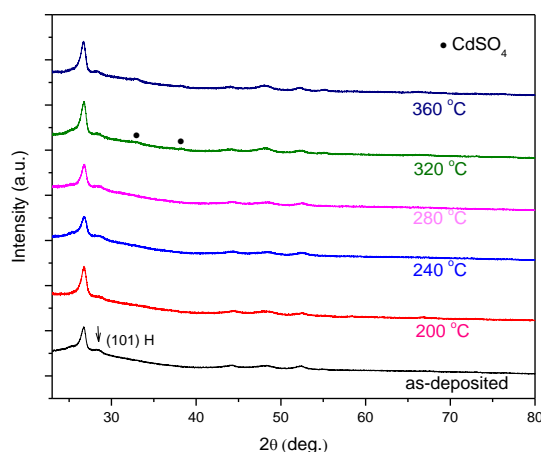


Fig. 1. XRD pattern of CdS film as-deposited and air-annealed at different temperatures.

Samples annealed in air at 360 °C ( $R_{360}$ ) show the peaks at angle  $2\theta=26.7028^\circ$ ,  $43.9556^\circ$ ,  $52.2552^\circ$ ,  $55.1410^\circ$  and  $72.7174^\circ$  which belongs to the (101), (220), (311), (222) and (420) planes, respectively, (ref. 01-075-0581). Only a small peak at angle  $2\theta = 48.1261^\circ$  belongs to the plane (103) was detected and this peak is related to the hexagonal CdS (ref: 00-041-1049).

The above analysis indicates that the samples as-deposited and annealed in air are polycrystalline in nature. It is also a mixture of hexagonal phase and cubic phase of CdS. There is a preferred orientation that is (111) in all cubic phases. The preferred (111) orientation was observed. This is because of controlled nucleation route in developed thin film samples. This indicates slow growing rate in film deposition [20, 21].

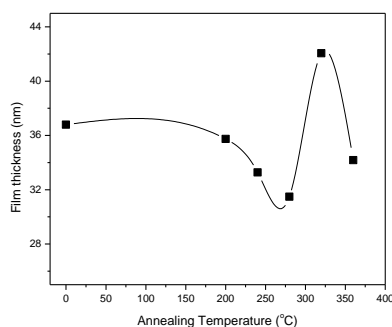


Fig. 2. Variation of film thickness with at different annealing temperatures.

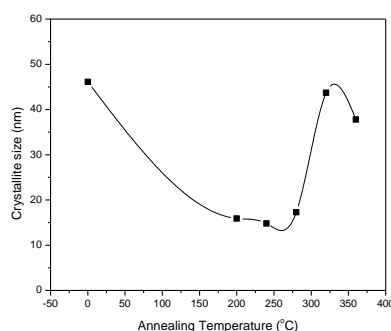


Fig. 3. Variation of crystallite size at different annealing temperatures.

The thickness of as-deposited thin film sample ( $R_0$ ) was found 36.8 nm and is reduced to 35.8, 33.3 and 31.5 nm when annealed in air at 200, 240 and 280 °C, respectively. The sample has maximum thickness only at the annealing temperature of 360 °C as shown in Fig. 2.

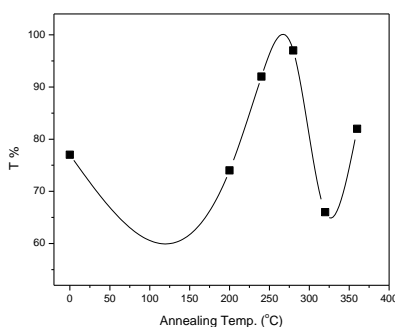


Fig. 4. Variation of T% at different annealing temperatures.

Crystallite size of as-deposited thin film sample ( $R_0$ ) is 46 nm as shown in Fig. 3. This crystallite size reduces to the average value of about 15.5 nm and remains about constant for the annealing temperature of 200, 240 and 280 °C. The crystallite size increases to a value of 43.7 nm at the annealing temperature of 320 °C and is reduced to 37.5 nm at 360 °C annealing temperature. This indicates the reduction in crystallite size while increasing temperature (annealing). This suggests to increase in crystallinity with increasing temperature (annealing).

Transmittance spectra (T %) of thin CdS thin films were recorded. The range of the recorded spectra was from 350 to 1100 nm as shown in Fig. 4. Transmittance Spectra show dependence of T% on  $\lambda$  at different temperature as shown in Fig. 4. Transmittance is 77 % at of 525 nm wavelength for the thin film as-deposited sample  $R_0$  and is about constant at this value for the sample ( $R_{200}$ ) annealed at a temperature of 200 °C.

Transmittance is about 92 % for the sample ( $R_{240}$ ) annealed at 240 °C and is increased to a maximum value of 97 % for the sample ( $R_{280}$ ) at the annealing temperature 280 °C. This maximum value of Transmittance is reduced to a value 66 % at the annealing temperature of 320 °C but increased to 82 % for the annealing temperature of 360 °C. It is observed the transmission spectra shifts to lower wavelength ( $\lambda$ ). This transferal of spectra shows increase in the optical  $E_g$  as shown in Fig. 7 and slightly decreases at the higher annealing temperature.

The dependence of optical absorption coefficient ( $\alpha$ ) on wavelength at 200, 240, 280, 320 and 360 °C annealing temperatures is shown in Fig. 5 and Fig. 6. Graph of  $(\alpha h\nu)^2$  against  $h\nu$  gives the value of  $E_g$ . Optical  $E_g$  is 2.68 eV for the as-deposited sample ( $R_0$ ) and slightly reduces to a value of 2.67 eV for sample annealed at 200 °C. This value of  $E_g$  further reduces to a value 2.59 eV for the sample  $R_{240}$  annealed at 240 °C. It was observed that the value of  $E_g$  is increasing in for the samples  $R_{280}$  annealed at 280 °C. This value is 2.70 eV. This value is further reduced to 2.63,

2.51 eV for the annealing temperature of 320 and 360 °C, respectively. Urbach-energy ( $E_u$ ) is shown in *Fig. 7*. Urbach-energy ( $E_u$ ) is also considered as band-tail-width. This band-tail-width is because of disorder in the thin-film material.

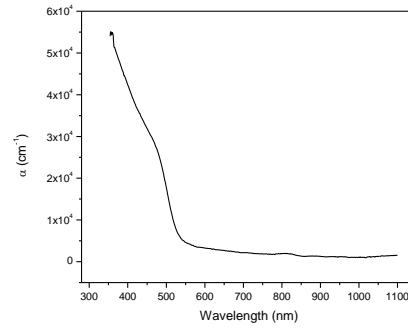


*Fig. 5. Dependence of  $\alpha$  on wavelength at 280 °C annealing temperature.*

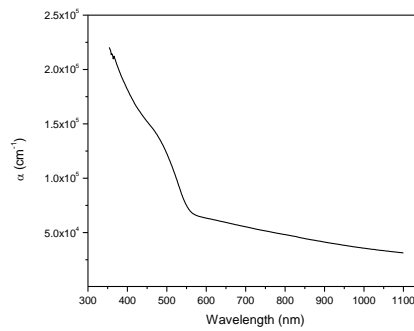


*Fig. 6. Dependence of  $\alpha$  on wavelength at 320 °C annealing temperature*

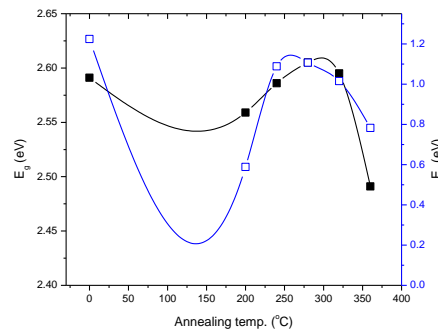


*Fig. 7. Dependence of  $E_g$  and  $E_u$  at different annealing temperatures.*

Disorder in the crystalline-material from the standard value is due to the variation of bond length and bond angle [23]. It is evident that optical  $E_g$  is reverse phenomenon to disorder. This behavior specifies that achieved optical  $E_g$  is administrated with the variation of disorder in CdS films.

#### 4. Conclusions

The grown CdS thin films were developed through chemical bath deposition technique at different temperatures. XRD analysis reveals that the CdS thin films indicates the presence of cubic phase. It is observed that the hexagonal structure were present at all temperatures. The size of crystallite was changed with temperature. The optical  $E_g$  was administrated with the disordering phenomenon in CdS thin films. The optical transmittance varied with the temperature.

#### References

- [1] H. Tanushevski, H. Osmani Chalcogenide Letters **15**(2), 107 (2018).
- [2] S. Mokrushin, Y. Tkachev, Z. Kolloidn, **23**, 438 (1961).
- [3] G. Kitaev, A. Uritskaya, S. Mokrushin, Russ.J. Phys.Chem. **39**, 1101 (1965).
- [4] A. V. Feitosa, M. A. R.Miranda, J. M. Sasaki, M. A. Araujo-Silva, Brazilian Journal of Physics **34**(2B), 656(2004).
- [5] H. Khallif, I. O. Oladej, L. Chow, Thin Solid Films **516**, 5967 (2008).
- [6] I. Oladeji, L. Chow, C. Ferekides, V. Viswanathan, Z. Zhao, Sol. Energy Mater. Sol. Cells **61**, 203 (2000).
- [7] Jiankang Li Ceramics International**41**(Supplement 1), July S376 (2015).
- [8] S. Vishnoi, R. Kumar, B. P. Singh, Journal of Intense Pulsed Lasers and Applications in Advanced Physics **4**(1), 35 (2014).
- [9] M. Becerril-Silva, O. Portillo-Moreno, R. Lozada-Morales, J. L. Fernandez-Muñoz, O. Zelaya-Ángel, Journal of Non-Oxide Glasses **9**(1), 1(2017).
- [10] T. L. Chu, S. S. Chu, C. Ferekides, C. Q. Wu, J. Britt, C. Wang, J. Cryst. Growth **117**(1-4), 1073 (1992).
- [11] C. Ferekides, J. Britt, Sol. Energy Mat. Sol. Cells **35**, 255 (1994).
- [12] I. Kaur, D. K. Pandya, L. Chopra, J. Electrochem. Soc. **127**, 943 (1980).
- [13] M. Froment, D. Lincot, Electrochim. Acta**40**, 1293 (1995).
- [14] J. F. Mohammad, Journal of Non - Oxide Glasses **10**(1), 27 (2018)
- [15] Z. Rizwan, B. Z. Azmi, M. G. M. Sabri, Optoelectron. Adv. Mat.**5**(4), 393 (2011).
- [16] A. S. Nazir, Z. Imran, A. Malik, M. Nazir, M. W. Ashraf, S. Tayyaba Digest Journal of Nanomaterials and Biostructures **13**(1), 307 (2018).
- [17] M. Caglar, Y. Caglar, S. Ilcan, J.Optoelectron.Adv. M.**8**(4), 1410 (2006).
- [18] D. Quinonez-Urias, Optical Materials Express **4**(11), 2280 (2014).
- [19] M. V. Kurik, Phys. Status Solidi. **A8**, 9 (1971).
- [20] K. R. Murali Mary Mathelinea Rita Johnb Chalcogenide Letters **6**(9) 483 (2009).
- [21] S. Soundswarm, O. SenthilKumar, R. Dhanasekaran, Mater.Lett.**58**, 2381 (2004).
- [22] G. C. Morris, R. Vanderveen, Sol. Energy Mater. Sol. Cells **27**, 305 (1992).
- [23] G. Sasikala, P. Thilakan, C.Subramanian, Sol. Energ. Mat. & Sol. C **62**, 275 (2000).
- [24] E. G. Mornani, P. Mosayebian, D. Dorranean, K. Behzad, Journal of Ovonic Research **12**(2), 75 (2016).
- [25] V. S. Sai Kumar, K. V. Rao, Journal of Optoelectronics and Biomedical Materials **9**(1), 27 (2017).
- [26] Fangyang Liu, Yanqing Lai JunLiu, Bo Wang, Sanshuang Kuang, Zhian Zhang, Jie Li Yexiang Liu Journal of Alloys and Compounds **493**, 305 (2010).
- [27] H. Moualkia, S. Hariech, M.S. Aida, Thin Solid Films **518**, 1259 (2009).